INVESTIGATION AND ANALYSIS OF INTERLEAVED DC-DC CONVERTER FOR SOLAR PHOTOVOLTAIC MODULE

S.SANKAR* and M.KUMARAN **

Professor in Department of EEE, SINCET,Nagapattinam,sankarphd@yahoo.com*

Professor in Department of EEE, Anand Institute of Higher Technology, Chennai, kumaranm.eee@aiht.ac.in**

Abstract: Solar energy is derived from solar radiations that are replaced constantly. A Conventional dc-dc Converter is suggested for very effective solar energy systems. It is not capable for obtain a high voltage gain even extreme duty cycle maintain the triggering circuit diagram. In order to increase the voltage gain for the new Boost converter from the solar power application. This paper presents a novel High Step-up Ratio Interleaved DC-DC Converter for Solar Photovoltaic Module. The advantages of interleaved boost converter related to the conventional boost converter are low input current ripple, high efficiency, faster transient response, reduced electromagnetic emission and improved reliability. The output voltage is high and voltage stress across the active switch is minimized and output ripples also minimized. The waveforms of input, inductor current ripple and output voltage ripple are achieved using MATLAB/Simulink

Key words— DC-DC Converter, Coupled Inductor, Solar photovoltaic system

1. Introduction

In Recent Years, wide use of electrical equipment has forced strict demands for electrical utilizing energy and this development is constantly growing. Accordingly, researchers and governments worldwide have prepared on renewable energy applications for explanatory natural energy consumption and environmental location. Among different renewable energy sources, the photovoltaic cell and fuel cell have been considering attractive choice. However, without additional arrangements, the output voltages generated from both sources. Thus, a high step-up dc-dc converter is desired in the power conversion systems corresponding to these two energy sources. In addition to the mentioned applications, a high step-up dc-dc converter is also required by many industrial applications, such as high-intensity discharge lamp ballasts for automobile headlamps and battery backup systems for uninterruptible power supplies [1].

The conventional boost converter can be advantageous for Step-up applications that do not demand very high voltage gain, mainly due to the resulting low conduction loss and design simplicity. Theoretically, the boost converter static gain tends to be infinite when duty cycle also tends to unity. However, in practical terms, such gain is limited by the I^2R loss in the boost inductor due to its intrinsic resistance, leading to the necessity of accurate and high-cost drive circuitry for the active switch, mainly because great variations in the duty cycle will affect the output voltage directly [2].

To achieve a high step-up voltage ratio, transformer- and coupled-inductor-based converters are usually the right choices. Compared with an isolation transformer, a coupled inductor has a simpler winding structure, lower conduction loss, and continuous conduction current at the primary winding, resulting in a smaller primary winding current ripple and lower input filtering capacitance. Thus, a coupled-inductor based converter is relatively attractive because the converter presents low current stress and low component count. However, for applications with low input voltage but high output voltage, it needs a high turn's ratio and its leakage inductor still traps significant energy, which will not only increase the voltage stress of the switch but also induce significant loss. Several methods have been proposed to solve these problems. A resistor–capacitor diode snubber can alleviate the voltage stress of the switch, but the energy that is trapped in the leakage inductor is dissipated.

In the converters that are operated in discontinuous-conduction mode boundary can reduce voltage stress. However, they will result in high input current ripple and require relatively large input and output filters. A passive lossless clamped circuit can recover the energy that is trapped in the leakage inductor and reduce voltage spike, but the

active switch is still in hard switching [3], [4].

The additional snubbers are required to reduce the voltage stresses of switches. In order to raise the efficiency and increase power conversion density, the soft-switching technique is required in dc/dc converters [5]. The high switching frequency used in static power converters can reduce the weight and size of the passive components. However, the switching losses on power semiconductors are also increased. The soft-switching techniques with variable switching frequency have been proposed to increase the switching frequency, reduce the size of power converters, and reduce the switching losses of the switching devices. The asymmetrical pulse width modulation (PWM) techniques were proposed in to achieve the zero-voltage switching (ZVS) feature at the power switch turn on instant. The active clamp techniques were presented in to achieve ZVS turn-on. Switching mode power supplies based on the fly back converter were widely used in industrial products for low-power applications. [6]. In the fly back converter, the transformer is adopted to achieve circuit isolation and energy storage. The zeta converters have been studied in to provide the isolated output voltage or achieve power factor correction. However, the power switch is operated in hard-switching PWM so that the circuit efficiency is low. The zeta converters with zero-current switching or ZVS technique have been proposed to reduce converter volume, voltage stresses of switching devices, and switching losses.

An asymmetrical interleaved high step-up converter that combines the advantages of the aforementioned converters is proposed, which combined the advantages of both. In the voltage multiplier module of the proposed converter, the turn's ratio of coupled inductors can be designed to extend voltage gain, and a voltage-lift capacitor offers an extra voltage conversion ratio.

Multi cascaded sources arrangement and this topology the source series from another source attached to a basic dc/dc converter is used to supply load power. Moreover a fraction of power from the source is passed through the converter suffering from conversion losses, and they remain power is supplied directly to the output load that does not have any power loss. Therefore, the source cascaded topology can achieve high-efficiency and high-voltage gains. In addition, due to this cascaded characteristics, the volume of transformer based on the voltage and current stress on some components of the basic converter, can likewise be reduced.

Literature review that has been done author used in the chapter "Introduction" to explain the difference of the manuscript with other papers, that it is innovative, it are used in the chapter "Research Method" to describe the step of research and used in the chapter "Results and Discussion" to support the analysis of the results [2]. If the manuscript was written really have high originality, which proposed a new method or algorithm, the additional chapter after the "Introduction" chapter and before the "Research Method" chapter can be added to explain briefly the theory and/or the proposed method/algorithm [4].

2. Interleaved Boost Converters

Interleaved buck and boost converters have been studied in recent years with the goal of improving power-converter performance in terms of size, efficiency, conducted electromagnetic emission and also transient response. The gains of interleaving consist of high power potential, modularity and better reliability. Since the inductor is frequently the largest and heaviest component in a high-boost converter, the use of a coupled inductor as a substitute of multiple discrete inductors is potentially beneficial. The coupled inductors also offer additional benefits such as reduced core and winding losses as well as better input and inductor current ripple. Generalized steady-state analysis of multiphase IBCs has been previously reported. Useful design equations for continuous inductor current mode (CICM) operation of an IBC, including the effects of inductor coupling on the key converter performance parameters (inductor ripple current, input ripple current, and minimum load current requirement for achieving CICM operation), are detailed in Reports studying specific applications for coupled inductor topologies including soft switching, active clamping, and high power utilization are becoming more prevalent in the literature as understanding of their benefits increase. Coupled Inductor

Intentional core gaps are the main source of leakage flux in the energy storing inductor. Outside the windings, flux associated with leakage takes a shorter path (i.e., through the air) and is, therefore, uncoupled. Flux associated with mutual inductance travels through all the windings and large portion of which remains in the core. In the dc environment, where two windings share the dc current equally, a flux-canceling inverse coupled configuration is utilized by implementing windings having opposing polarity. At the core directly under the windings of

N turns each,

The Resultant flux is (1- k) LI0 /N.
Where, I_0 is dc current through the winding.

3. Performance Analysis of the Proposed Converter

The proposed interleaved high step up ratio Interleaved DC-DC boost converter as shown in Fig. The operation of the high step-up ratio interleaved DC-DC boost converter is explained as following four modes and the proposed converter has given on Fig 1.
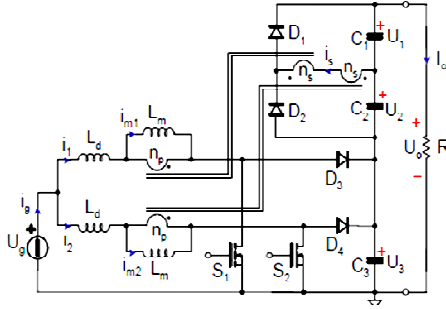

Fig 1. Proposed interleaved High Step-up Ratio Interleaved DC-DC boost converter

Mode 1 [*t*0, *t*1]: At $t = t0$, the power switch $S2$ remains in ON state, and the other power switch $S1$ begins to turn on. The diodes $Dc1$, $Dc2$, $Db1$, $Db2$, and $Df1$ are reversed biased, as shown in Fig. 5(a). The series leakage inductors Ls quickly release the stored energy to the output terminal via fly back–forward diode $Df2$, and the current through series leakage inductors Ls decreases to zero. Thus, the magnetizing inductor $Lm1$ still transfers energy to the secondary side of coupled inductors. The current through leakage inductor $Lk1$ increases linearly and the other current through leakage inductor $Lk2$ decreases linearly.

Mode 2 [*t*1, *t*2]: At $t = t1$, both of the power switches $S1$ and $S2$ remain in ON state, and all diodes are reversed biased, as shown in Fig. 5(b). Both currents through leakage inductors $Lk1$ and $Lk2$ are increased linearly due to charging by input voltage source Vin.

Mode 3 [*t*2, *t*3]: At $t = t2$, the power switch $S1$ remains in ON state, and the other power switch $S2$ begins to turn off. The diodes $Dc1$, $Db1$, and $Df2$ are reversed biased, as shown in Fig. 5(c). The energy stored in magnetizing inductor $Lm2$ transfers to the secondary side of coupled inductors, and the current through series leakage inductors Ls flows to output capacitor $C3$ via fly back–forward diode$Df1$.

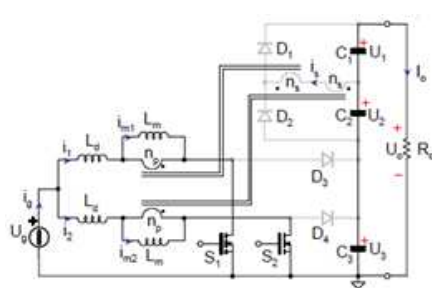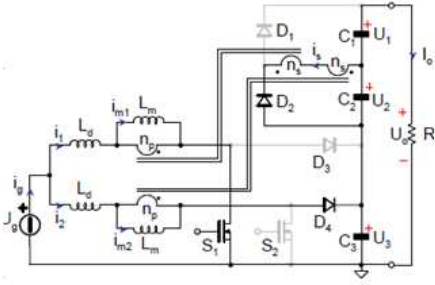Mode-1(T01 = t1-t0)
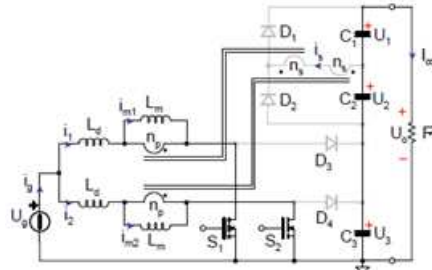
Mode-2(T12 = t2-t1)
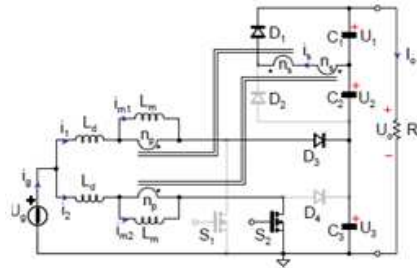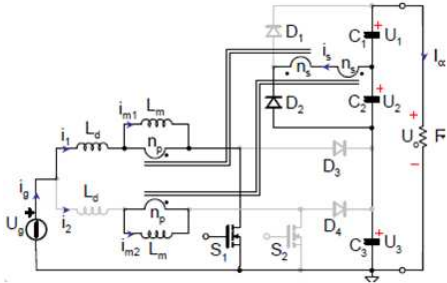

Mode-3(T23 = t3-t2)
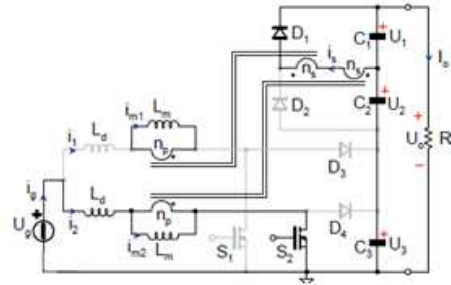
Mode-4(T34 = t4-t3)
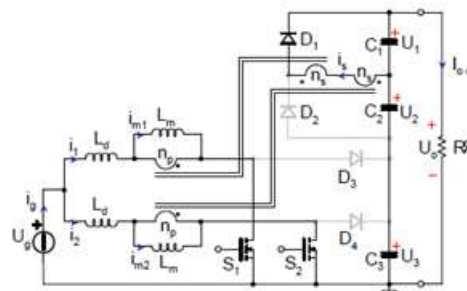
Mode-5(T45 = t5-t4)

Mode-6(T56 = t6-t5)
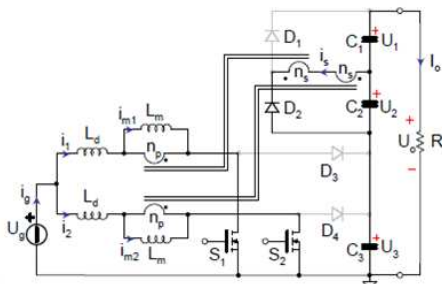

Mode-7(T67 = t7-t6)

Mode-8(T78 = t8-t7)

Fig 2.Operating modes of the proposed converter

The voltage source, magnetizing inductor $Lm2$, leakage inductor $Lk2$, and clamp capacitor $Cc2$ release energy to the output terminal; thus, $VC1$ obtains a double output voltage of the boost converter.

Mode 4 [*t3, t4*]*:* At $t = t3$, the current $iDc2$ has naturally decreased to zero due to the magnetizing current distribution, and hence, diode reverse recovery losses are alleviated and conduction losses are decreased. Both power switches and all diodes remain in previous states except the clamp diode $Dc2$, as shown in Fig. 5(d).

Mode 5 [*t4, t5*]*:* At $t = t4$, the power switch $S1$ remains in ON state, and the other power switch $S2$ begins to Turn on. The diodes $Dc1$, $Dc2$, $Db1$, $Db2$, and $Df2$ are reversed biased, as shown in Fig. 5(e). The series leakage inductors Ls quickly release the stored energy to the output terminal via fly back–forward diode $Df1$, and the current through series

leakage inductors decreases to zero. Thus, the magnetizing inductor $Lm2$ still transfers energy to the secondary side of coupled inductors. The current through leakage inductor $Lk2$ increases linearly and the other current through leakage inductor $Lk1$ decreases linearly.

Mode 6 [*t5, t6*]*:* At $t = t5$, both of the power switches $S1$ and $S2$ remain in ON state, and all diodes are reversed biased, as shown in Fig. 5(f). Both currents through leakage inductors $Lk1$ and $Lk2$ are increased linearly due to charging by input voltage source Vin.
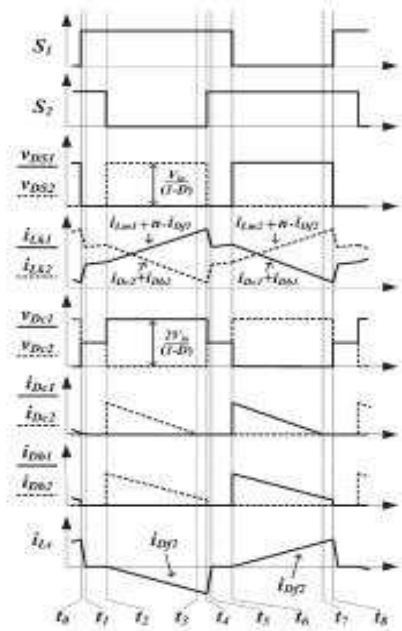
Fig 3.Firing Pulses for Switch1 and Switch2

Mode 7 [*t6, t7*]*:* At $t = t6$, the power switch $S2$ remains in ON state, and the other power switch $S1$ begins to turn off. The diodes $Dc2$, $Db2$, and $Df1$ are reversed biased, as shown in Fig. 5(g). The energy stored in magnetizing inductor $Lm1$ transfers to the secondary side of coupled inductors, and the current through series leakage inductors flows to output capacitor $C2$ via fly back–forward diode $Df2$. The voltage stress on power switch $S1$ is clamped by clamp capacitor $Cc2$ which equals the output voltage of the boost converter.

The input voltage source, magnetizing inductor $Lm1$, leakage inductor $Lk1$, and clamp capacitor $Cc1$ release energy to the output terminal; thus, $VC1$ obtains double output voltage of the boost converter.

Mode 8 [*t7, t8*]*:* At $t = t7$, the current $iDc1$ has naturally decreased to zero due to the

magnetizing current distribution, and hence, diode reverse recovery losses are alleviated and conduction losses are decreased. Both power switches and all diodes remain in previous states except the clamp diode $Dc1$, as shown in Fig. 5(h).

4. Simulation Results

Based on the above analysis the step up DC – DC converter is have to obtain the more voltage gain for the required voltage rating for the solar power application with proper design of all the parameter of the circuit diagram. With a help of modified capacitor in order to increase the voltage rating and reduce the ripple content in the output side of the converter, the proposed converter is shown in Fig 1. In this circuit have modified Coupled Inductor and Capacitor for getting high voltage gain from the simulation circuit of Fig.4, It shows that the overall circuit diagram of the simulated proposed converter Circuit diagram using the MATLAB SIMULINK software tool. In this result of input and output waveforms are obtain separately as shown in Fig 5 to Fig 10.
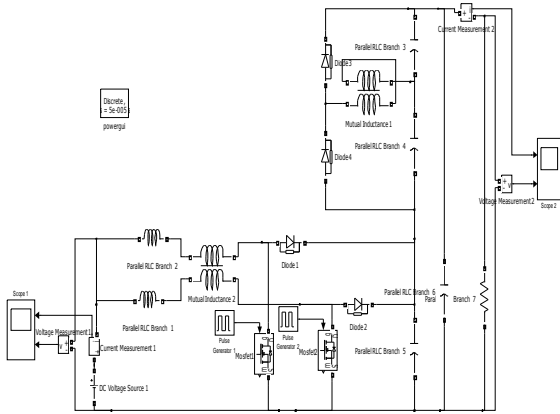
Fig 4. MATLAB/SIMULINK circuit diagram of the proposed DC-DC converter Simulation.
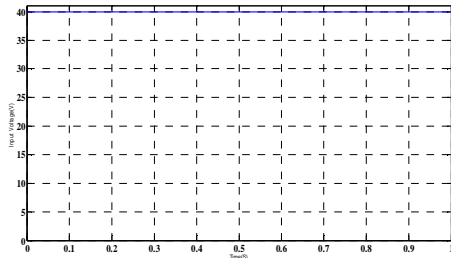
Fig.5.Input Dc voltage of Proposed Converter
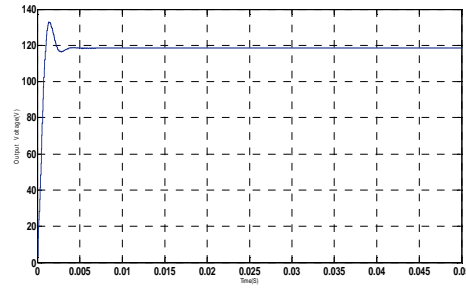
Fig 6 . output voltage of proposed converter.
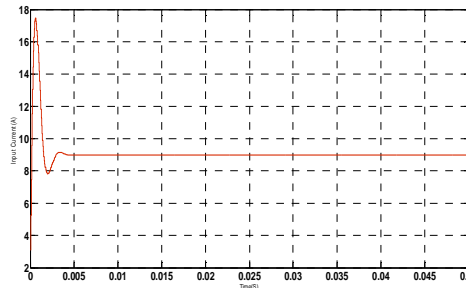
Fig 7. Input Current of proposed converter
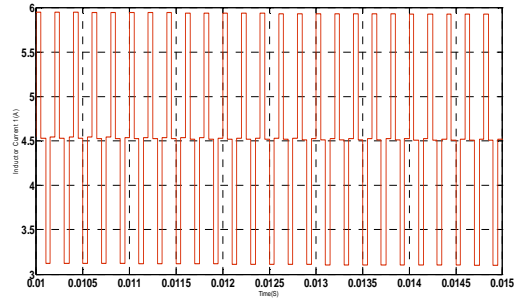
Fig 8.Current through the inductor 1
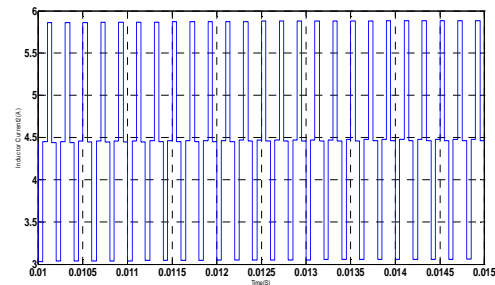
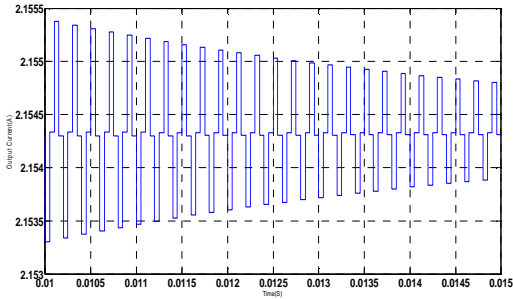Fig 9 .Current through the inductor 2

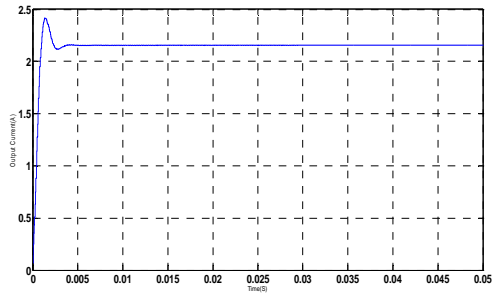Fig 10(a). Output Current of proposed converter

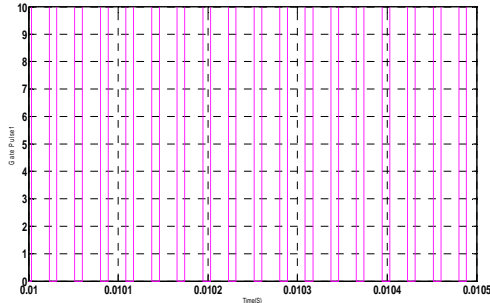Fig 10(b). Output Current of proposed converter
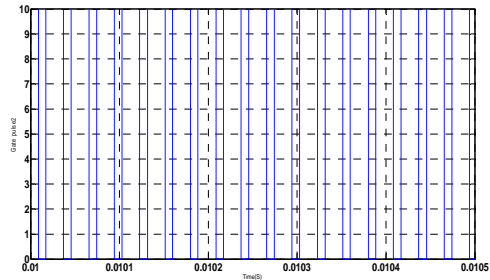

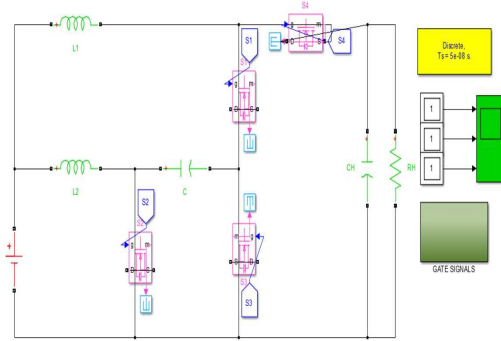Fig 11.Firing pulses for switch1

Fig 11.Firing pulses for switch2

Fig -12: Simulink model of converter in step-up mode

The voltage and current waveforms of electrical components of the converter in step down operation mode is shown below. Here the output voltage is fixed at 2.5V that is even if we vary the input voltage the output voltage does not change.
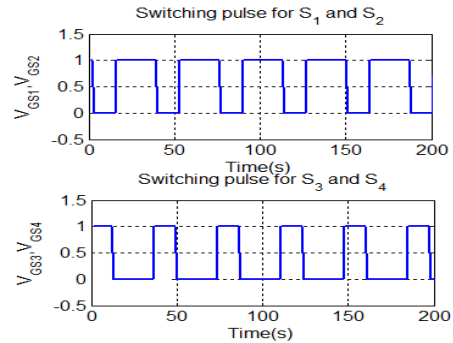

Fig.13. Switching pulse

Fig-13 shows the switching pulses for the four switches. Fig-14 shows the input voltage in step-down mode and it is 25V. Output voltage is shown in Fg-15. For an input voltage of 25V, output voltage is obtained as 2.5V. Fig-16shows the current through the inductors $L_1$and L_2 in step-down mode. The voltage waveforms of switches in step-down mode are shown in Fg-17.
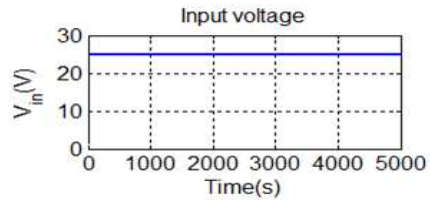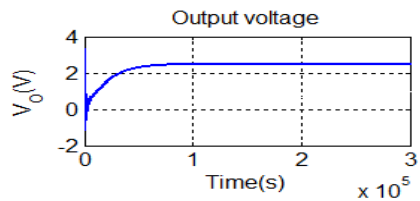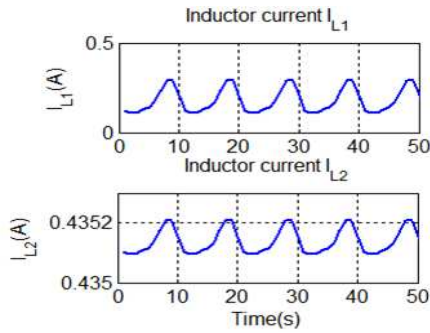

Fig .14. Input voltage

Fig.15.Output voltage

Fig.16 Inductor current

As shown in the fig-17, the current of inductors L_1 and L_2 are about 0.2A and 0.45A, respectively, in step-dwn mode. From the waveform of voltage stress $V_{S1} = V_H = 25V$, $V_{S2} = V_{S3}$ equal to square root of V_L and V_H which is equal to 7.9V and V_{S4} is sum of V_{S2} and V_H is equal to 32.9V are obtained.
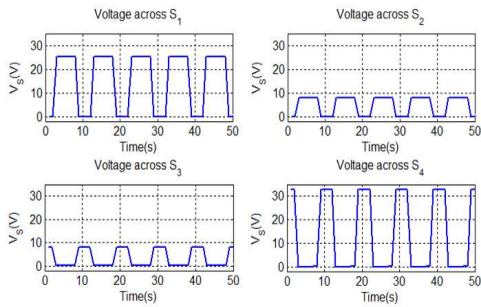

Fig.17. Voltage stress

Fig-18 shows the input voltage in step-up mode and it is 2.5V. Output voltage is shown in Fg-19. For an input voltage of 2.5V, output voltage is obtained as 25V. Fig-20 shows the current through the inductors L_1 and L_2 in step-down mode. The voltage waveforms of switches in step-down mode are shown in Fg-21.
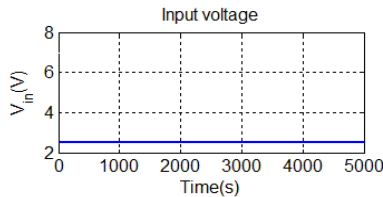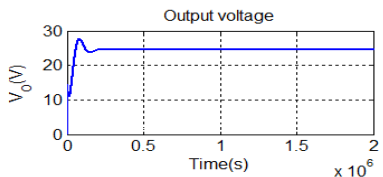

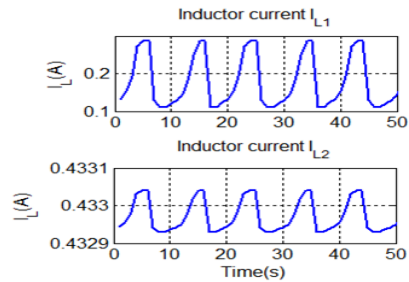Fig.18.Input voltage

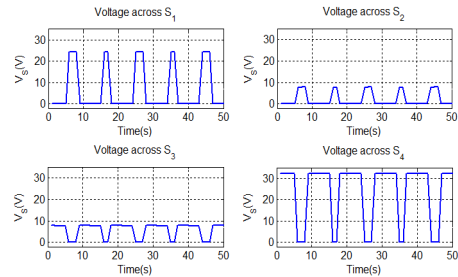Fig.19 .Output voltage

Fig.20. Inductor current

Fig.21. Voltage stress

5. Experiment Setup and Results

The experiment setup is shown in Fig-22, IRFP260 and IRFP460 are used as switches. The controller used in the prototype is dsPIC30F2010. The hardware results are shown below; Output pulse from driver IC which is of 12V is shown in Fig-23. In the Fig-24 shows the input and output voltage in the step-down mode. In the step-down mode a gain of 0.1 is obtained and the Fig-25 shows the input and output voltage in the step-up mode and in this mode a gain of 5 is obtained.
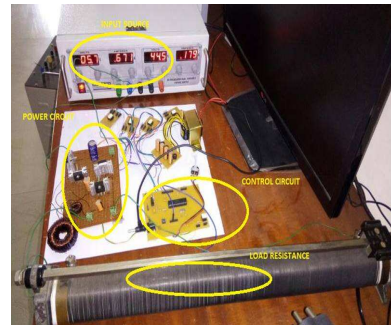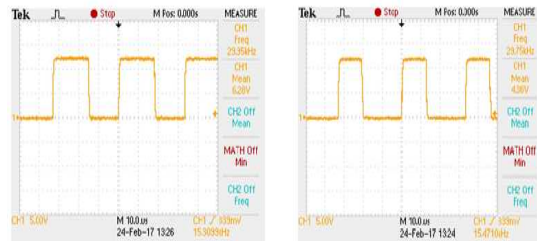

Fig.22. Experiment setup
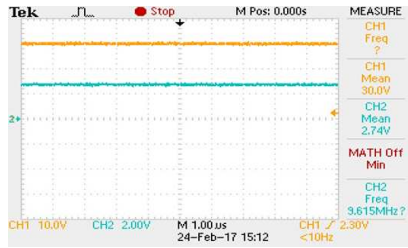

Fig.23. Output of TLP250

Fig.24. Input and output voltage of step-down mode
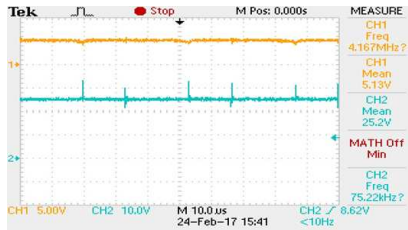

Fig.25. Input and output voltage of step-up mode

TABLE I. Design Considerations of Proposed Converter.

S.NO	PARAMETER	VALUES
1.	Input voltage	60V
2.	Capacitor (C1)	30µF/300V
3.	Capacitor (C2)	30µF/600V
4.	Diodes	0 .7V
5.	Switching frequency	45KHZ
6.	Load resistance	400Ω
7.	Self inductance	10µH
8.	Mutual inductance	5µH
9.	Turn's ratio (n2:n1)	1:1
10.	Output voltage	600V
11.	Output power	900W

6. **Conclusion**

An optimized genetic algorithm method was presented to solve the optimal power flow problem of power system with FACTS devices. The proposed method introduces the injected power model of FACTS devices into a conventional AC optimal power flow problem to exploit the new characteristic of FACTS devices. Case studies on modified IEEE test system show the potential for application of OGA to determine the control parameter of the power flow controls with FACTS. In this method, OGA effectively finds the optimal setting of the control parameters using the conventional OPF method. It also shows that the OGA was suitable to deal with non-smooth, non-continuous, non-differentiable and non-convex problem, such as the optimal power flow problem with FACTS devices.

Reference

1. Report IEA-PVPS T5-01: Utility Aspects of Grid Connected Photovoltaic Power Systems; 4. AC-MODULE, pp. 4-19.

2 S.B Kjaer, J.K. Pedersen, F. Blaabjerg, "A review of singlephase grid-connected inverters for photovoltaic modules", IEEE Transactions on Industry Applications, Vol. 41, Issue 5, pp. 1292–1306, October 2012.

3 J. M. A. Myrzik, M. Calais, "String and module integrated inverters for single-phase grid connected photovoltaic systems", IEEE Power Tech Conference Proceedings, Bologna, Vol. 2, pp. 8, 23-26, June 2014.

4 M. Byung-Duk, L. Long-Pil, K. Jong-Hyun, K. Tae-Jin, Y. Dong-Wook, R. Kang-Ryoul, K. Jeong-Joong, S. Eui-Ho, "A Novel Grid-Connected PV PCS with New High Efficiency Converter", Journal of Power Electronics, Vol. 8, No. 4, pp. 309- 316, October 2015.

5 C. Gyu-Ha, K. Hong-Sung, H. Hye-Seong, J. Byong-Hwan, C. Young-Ho, K. Jae-Chul, "Utility Interactive PV Systems with Power Shaping Function for Increasing Peak Power Cut Effect", Journal of Power Electronics, Vol. 8, No. 4, pp. 371-380, October 2015.

6 N. Denniston, A. M. Massoud, S. Ahmed, and P. N. Enjeti, "Multiplemodule high-gain high-voltage DC–DC transformers for offshore wind energy systems," IEEE Trans. Ind. Electron., vol. 58, no. 5, pp. 1877– 1886, May 2015